



Anelasticity of die-cast magnesium-aluminium based alloys under different strain rates



Hua Qian Ang^a, Trevor B. Abbott^{a,b}, Suming Zhu^a, Mark A. Easton^{a,*}

^a School of Engineering, RMIT University, Bundoora, Victoria 3083, Australia

^b Magontec Limited, Sydney, New South Wales 2000, Australia

ARTICLE INFO

Keywords:

Magnesium alloys
Anelasticity
Twinning
Strain-rate sensitivity
High-pressure die-casting

ABSTRACT

Cyclic tension loading-unloading tests were conducted over a wide quasi-static strain rate range $10^{-6} - 10^{-1} \text{ s}^{-1}$ on a variety of die-cast Mg-Al based alloys, from which the deformation behaviour, especially the anelasticity, has been systematically studied. At the early stages of deformation, prior to the onset of extensive prismatic slip, the anelastic strain is less dependent on strain rate but varies between the alloys. Upon the activation of extensive prismatic slip, the anelastic strain starts to saturate at a maximum. The maximum increases with increasing strain rate and varies between alloys. The strain-rate dependence of the maximum anelastic strain can be interpreted in terms of solid solution softening/hardening of slip planes and their influence on twinning. Implications of the strain-rate dependence of anelasticity on proof stress measurement of Mg alloys are also discussed.

1. Introduction

The deformation behaviour of magnesium (Mg) alloys is complex due to limited dislocation slip systems [1], leading to difficulties in measuring yield strength [2] and perceived limits to ductility. The limited slip systems results in the activation of twinning to accommodate plastic deformation and the stress-strain curves can be divided into several segments [3–5]. Initial deformation is elastic (stage I) followed by a non-linear region (stage II) in which basal slip and twinning are the dominant deformation mechanisms [6–10]. The twins formed in this region are not stable [11] and can revert during unloading [12], making a large part of stage II deformation reversible. At higher stresses, deformation via prismatic slip takes place leading to extensive plastic deformation (stage III) [3,13]. Eventually the onset of dynamic recovery via the activation of pyramidal slip leads to the final stage of deformation before fracture (stage IV) [13–15].

The focus of this paper is on the reversible component of stage II deformation. The terms anelastic and pseudo-elastic have been used in the past to describe this component [16–20]. The study of anelasticity in stage II is important as it influences several properties including yield strength [2], fatigue strength [21], apparent stiffness [16,17] and sound dampening [11]. The anelastic behaviour of Mg alloys, which manifests as hysteresis loops in loading-unloading stress-strain curves, has been observed in pure Mg and Mg-Zn alloys [17], Mg-Al alloys [22], AZ31 (Mg-3Al-1Zn) [9], AZ91 (Mg-9Al-0.6Zn) [16], AM60B (Mg-6Al-0.3Mn)

and AE44 (Mg-4Al-4RE) [21].

This study focuses on high-pressure die-cast alloys. Die-cast alloys account for the large majority of Mg alloy usage and anelasticity contributes significantly to deformation due to the fine grain size. Experiments on pure Mg [23] and die-cast AZ91 [16] have shown that the anelastic effect is more significant in fine-grained alloys. The increase in anelasticity in fine-grained AZ91 was attributed to the formation of fine and unstable twins, which are more prone to revert upon unloading [16]. Anelasticity is also influenced by solute content. The largest anelastic effect has been observed in pure Mg and decreased with increasing Zn [17] and Gd [19] solute concentrations. It was proposed that introduction of solute in solution can lower the critical resolved shear stress (CRSS) for prismatic slip. Consequently, twinning becomes less necessary during deformation, lowering the amount of reversible twinning. Although there was a monotonic decrease in anelasticity with increasing Zn and Gd contents, a similar trend was not observed in Mg-Al alloys; both Mg-0.5Al and Mg-2Al alloys showed similar anelasticity despite the difference in Al content [22]. However, the study was complicated by the fact that the grain size of the Mg-0.5Al alloy was three times larger than that of the Mg-2Al alloy. Anelasticity of Mg alloys has also been observed to be more pronounced in compression than in tension [16,17], due to increased activity of $\{10\bar{1}2\}$ twinning [24].

Recently, the effects of strain rate on the tensile properties and deformation microstructures of a range of Mg die-casting alloys

* Corresponding author.

E-mail address: mark.easton@rmit.edu.au (M.A. Easton).

including AM40 (Mg-4Al-0.3Mn), AM60, AZ91, and AE44 (as cast and T5 aged) have been studied by the present authors over a wide strain rate range 10^{-6} – 10^{-1} s^{-1} [25]. It was shown that strain-rate sensitivity decreases with increasing Al solute level in the alloys, due to dynamic strain ageing from the interaction between Al solute and dislocations. It was also shown that deformation twinning is more active in alloys with higher Al solute levels.

The focus of the present work is on the anelastic behaviour of Mg die-casting alloys under a similar strain rate range. The selection of these alloys was influenced in part by their use as commercial alloys, but principally to examine a range of alloy behaviours. AM40, AM60 and AE44-F have moderate strength but good ductility, while AZ91 and AE44-T5 are higher-strength alloys. The strengthening mechanisms within these two alloys are very different with AE44-T5 strengthened by nanoscale precipitates [26] while AZ91 is strengthened, at least in part, by an intermetallic skeleton [27,28]. Comparisons of the amount of anelasticity in these alloys can yield insights into the deformation mechanisms.

2. Materials and experimental details

Mg alloys AM40, AM60, AZ91 and AE44 were high-pressure die-cast in a 250 ton cold chamber machine. More details about the casting process can be found elsewhere [29]. The chemical compositions of these alloys were analysed by inductively coupled plasma atomic emission spectroscopy (ICP-AES) and are listed in Table 1. AE44 specimens were also given an ageing treatment for 32 h at 200 °C (labelled T5).

Cast-to-size cylindrical cross section, dog-bone shaped tensile samples, 100 mm in length with a 36 mm parallel section in the gauge length and a diameter of 5.6 mm were used in this study. Monotonic and cyclic tension loading-unloading tests were performed on an Instron 5569 universal testing machine with a 50 kN load cell at room temperature using a constant rate of crosshead displacement with nominal strain rates in the range from 10^{-6} to 10^{-1} s^{-1} . For the cyclic loading-unloading tests, the samples were loaded to a predetermined strain, unloaded to zero stress and then reloaded again. All alloys were cyclically tested to 3% strain, except AZ91, which was tested to a higher strain (4.5%) in order to determine saturation of anelasticity. Each test was repeated at least twice to ensure reproducibility. Compression tests were not conducted in this study as high-pressure die-cast alloys are relatively isotropic in mechanical properties [30,31].

Deformation microstructures of AE44 after cyclic testing to 3% strain at different strain rates were characterised by electron-back-scattered diffraction (EBSD) and transmission electron microscopy (TEM). EBSD data was collected in a FEI Nova NanoSEM at 20 kV using a 0.5- μm step size. HKL Channel 5 Tango subroutine was used to identify the twinning types based on the misorientation angle/axis between the twinned region and matrix. They are $\{10\bar{1}2\}$ twins (i.e. $86^\circ < 12\bar{1}0 >$), $\{10\bar{1}1\}$ twins (i.e. $56^\circ < 12\bar{1}0 >$) and $\{10\bar{1}3\}$ twins (i.e. $64^\circ < 12\bar{1}0 >$) [32–34]. The surfaces of all samples for EBSD analysis were prepared using standard mechanical polishing procedures and were finished by 0.06 μm OP-S. For TEM, the foils were cut from tested specimens and were prepared by ion milling using a Gatan Precision Ion Polishing System (PIPS) at 4 keV with an incident angle of 4° . The thin foils were examined in a JEOL 2100F TEM.

Table 1
Chemical compositions (wt%) determined by ICP-AES for the studied die-cast Mg alloys.

Alloy	Al	Mn	RE (Ce + La)	Zn	Mg
AM40	4.44	0.21	< 0.01	0.05	Bal.
AM60	6.26	0.29	< 0.01	0.1	Bal.
AZ91	8.88	0.19	< 0.01	0.74	Bal.
AE44	3.67	0.31	3.83	< 0.01	Bal.

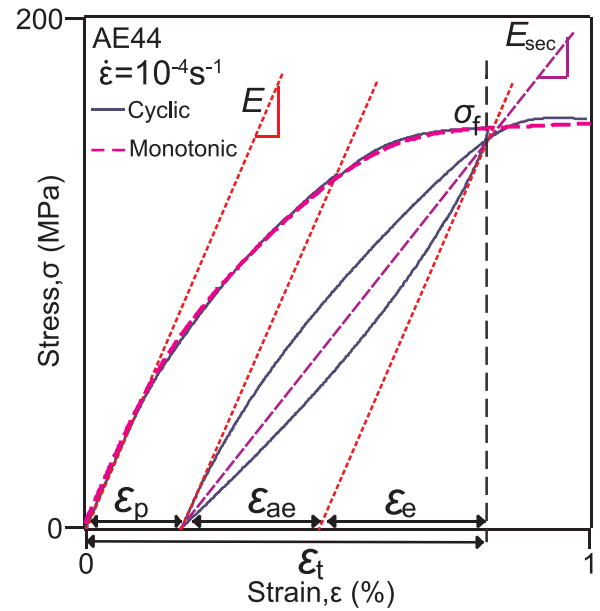


Fig. 1. An overview of cyclic stress-strain curve of die-cast AE44 at 10^{-4} s^{-1} , where the total strain (ϵ_t) can be separated into linear elastic strain (ϵ_e), anelastic strain (ϵ_{ae}) and plastic strain (ϵ_p). E is the nominal elastic modulus of Mg, taken as 45 MPa [38,39], while E_{sec} is the secant elastic modulus. σ_f is defined as the applied stress where unloading starts. The dashed line is the monotonic tensile flow curve.

3. Results

Fig. 1 shows a typical loading-unloading hysteresis loop for AE44 at 10^{-4} s^{-1} . Several relevant parameters are defined where the total strain (ϵ_t), is separated into three parts: linear elastic strain (ϵ_e), anelastic strain (ϵ_{ae}) and plastic strain (ϵ_p). Also shown is the corresponding monotonic flow curve. The monotonic flow curve follows closely the cyclic one, indicating that cyclic loading does not have an additional effect on the overall deformation behaviour.

Fig. 2(a) and (b) show the monotonic flow curves of AZ91 and AE44, respectively to illustrate the two extremes of behaviour observed in these experiments. The flow curves of as-cast AE44 consistently shift higher with increasing strain rate while the changes in the flow curves of AZ91 are marginal. The flow curves of aged AE44-T5 show slightly higher strain-rate dependence than that of AE44, while the flow curves of AM40 and AM60 behave more like AZ91, which show a much lower influence of strain rate. Cyclic flow curves (not shown) exhibit the same strain-rate effect as monotonic flow curves.

The monotonic flow curve can also be separated into different stages based on the Kocks-Mecking method of analysis [35,36] extended by Cáceres and his co-workers [3,13,37] for Mg polycrystals. Determination of these stages is illustrated in Fig. 2(c) and (d). Assuming the elastic fraction, f , of the alloy deforms with an elastic modulus, $E = 45 \text{ GPa}$ [38,39], and the plastically deforming fraction strain hardens at a rate of, $\Theta_h = 1.4 \text{ GPa}$ (pure Mg polycrystals) [3–5], f can be calculated [3]:

$$f = \frac{\frac{d\sigma}{d\epsilon} - \Theta_h}{E - \Theta_h} \quad (1)$$

Where σ and ϵ are true stress and strain, respectively. The alloys are fully elastic (stage I) up to $\sim 65 \text{ MPa}$ for AZ91 and $\sim 45 \text{ MPa}$ for AE44. The departure from pure elasticity indicates the onset of stage II. During stage II, the elastic fraction decreases rapidly due to basal slip and twinning [3–5,37,40,41] and possibly a small amount of prismatic slip. The elastic fraction reaches zero when the alloy becomes fully plastic due to extensive prismatic slip (stage III) [3]. The onsets of these stages are also shown in Fig. 2(a) and (b) and onset values reported in Table 2. Upon extensive activation of prismatic slip, the strain hardening rate

Download English Version:

<https://daneshyari.com/en/article/5455215>

Download Persian Version:

<https://daneshyari.com/article/5455215>

[Daneshyari.com](https://daneshyari.com)